Makara Journal of Technology

Volume 24 | Issue 3 Article 7

12-3-2020

Influence of the Shaping Process on the Tensile Properties of Steel Reinforcement Bars Carbon Steel Grades BJTP24 and BJTS40

Nuraziz Handika
Department of Civil Engineering, Faculty of Engineering, Universitas Indonesia, Depok 16424, Indonesia, n.handika@ui.ac.id

Ridha Amalia Idhar
Department of Civil Engineering, Faculty of Engineering, Universitas Indonesia, Depok 16424, Indonesia

Jessica Sjah
Department of Civil Engineering, Faculty of Engineering, Universitas Indonesia, Depok 16424, Indonesia

Essy Arijoeni
Department of Civil Engineering, Faculty of Engineering, Universitas Indonesia, Depok 16424, Indonesia

Elly Tjahjono
Department of Civil Engineering, Faculty of Engineering, Universitas Indonesia, Depok 16424, Indonesia

Makara J. Technol. 24/3 (2020), 139–148
doi: 10.7454/mst.v24i3.3914

Influence of the Shaping Process on the Tensile Properties of Steel Reinforcement Bars Carbon Steel Grades BJTP24 and BJTS40

Nuraziz Handika*, Ridha Amalia Idhar, Jessica Sjah, Essy Arijoeni, and Elly Tjahjono

Department of Civil Engineering, Faculty of Engineering, Universitas Indonesia, Depok 16424, Indonesia

**E-mail: n.handika@ui.ac.id*

Abstract

According to the current applicable national standard in Indonesia, i.e. SNI 07 2529 1991, in addition to the limitation on the loading rate, the steel bar must be reduced, formed, or lathed, as part of the shaping process of samples. This study determined and compared the effect of the shaping process on the yield strength, ultimate strength, and percent elongation by conducting tensile tests of steel bar grade BJTS40, i.e. deformed bar type of steel, and grade BJTP24, i.e., plain bar type of steel. Three diameters of the deformed bar (BJTS40) and one diameter of the plain bar (BJTP24) were used. Samples of the bars were taken randomly from a local distributor in the Greater Jakarta area. Each 1 m of the bar is divided into two, i.e. one end being the *non-shaped* sample and the other end being the *shaped* sample. Tensile tests of these two sides were conducted. This study determined that the shaping process influences the results of the tensile test, particularly the variation of percent elongation. Moreover, the effects of the shaping process can be inferred from the high coefficients of variation of yield strength (4.33%) and ultimate strength (2.40%) of the *shaped* sample. The results of this study, which elucidate the effects of the shaping process on tensile tests, can be used as an information resource in engineering practice.

Abstrak

Pengaruh Proses Pembentukan pada Sifat Tarik Besi Beton Kualitas Baja Karbon BJTP24 dan BJTS40. Menurut standar nasional yang berlaku di Indonesia, SNI 07 2529 1991, selain adanya batasan kecepatan pembebanan, sampel batang baja harus dikurangi, dibentuk, atau dibubut, sebagai bagian dari proses persiapan sampel. Penelitian ini membandingkan efek pembentukan proses pada uji tarik dari baja batangan mutu BJTS40 untuk baja tulangan sirip dan baja batangan mutu BJTP24 untuk baja tulangan polos terhadap tiga parameter utama baja yaitu: kekuatan leleh, kekuatan ultimit dan % perpanjangan. Tiga diameter baja tulangan sirip BJTS40 dan satu diameter baja tulangan polos BJTP24 digunakan. Sampel batang dipilih secara acak dari distributor local di wilayah Jakarta. Setiap satu metre batang dibagi menjadi dua, satu ujung tidak dibubut dan yang lainnya sampel yang dibubut. Hasil uji tarik dari sampel kedua sisi ini diamati. Berdasarkan studi ini, proses pembubutan mempengaruhi hasil uji tarik, khususnya pada koefisien variasi dari % perpanjangan. Selain itu, efek dari proses pembubutan juga dapat dilihat pada koefisien variasi yang lebih besar untuk tegangan leleh (4,33%) dan tegangan ultimit (2,40%) untuk sampel yang dibubut. Hasil penelitian ini bermanfaat sebagai sumber informasi dalam penggunaan praktis keteknikan dengan memberikan efek dari proses pembubutan pada sampel baja untuk tes tarik.

Keywords: elongation, failure mode, shaping process, steel bar properties, steel reinforcement bar

1. Introduction

As the most widely used material in the construction industry, concrete has high compressive strength but is relatively weak when subjected to tensile, flexural, or shear forces [1]–[3]. To overcome this weakness, a reinforcement bar (rebar) is cast as a tensioning device to reinforce concrete to withstand different tension states. The ideal material for rebar that is widely used in reinforced concrete (RC) is steel because of its properties. Steel has high tensile strength and bonds well with concrete compared with other materials [4].

Laboratory tensile tests on steel rebars should be conducted as one of the quality control procedures in construction. In the construction field, rebar is used as it is, without reducing, forming, or lathing the section. Nevertheless, the current applicable national standard in Indonesia, i.e. *Standar Nasional Indonesia* (SNI) 07 2529 1991 [5], recommends the so-called shaping process before laboratory tensile tests. The shaping process recommended in SNI 07 2529 1991 [5] follows the standard methods established in ASTM E8-04 [6]. In this standard, steel rod specimens used in tests should be either substantially full size or machined.

According to certified industries in Indonesia [7], during the finishing stage, the rebar undergoes a process called heat treatment, which is considered the final touch. However, heat treatment may affect the mechanical properties of the rebar. Moreover, the conditions of the outer and inner parts of the rebar may not be exactly homogenous. This situation is similar to the different temperature conditions encountered during the production process of thermomechanically treated (TMT) rebar [8]. Regarding this condition, the national standard recommends the shaping process to remove the outer part of the bar before the test.

The change in diameter due to the shaping process can influence the results of the tensile test of steel rebar. This shaping or machining process also influences the stress–strain curve of the bar. As the diameter decreases, the values of stress and strain also decrease. The same result is also obtained for yield strength, ultimate strength [9], [10], and modulus of elasticity of steel [9].

In terms of potential failure modes, ductile steel material exhibits ductile fracture, also called a cup-and-cone fracture, on the halves of the broken specimen. Ductile fracture occurs as a result of instability due to large local deformation. This type of fracture can have either a ductile or brittle global behavior depending on the density of the defects [11]. In the area with defects, stress concentration due to external load can lead to large plastic deformations. This condition creates the cavity that propagates to the final fracture.

The cup-and-cone fracture originates from a previously existing crack of the specimen and the shear plane. The previously existing crack of the sample itself is created when the specimen, particularly its perpendicular plane with rough and fibrous fracture surfaces, is subjected to tensile stress. The shear plane is created before the specimen breaks and is formed along the periphery of the sample at approximately 45° to the tensile test axis [12], [13]. However, the failure mode is not always the same for all samples during the tensile tests.

Furthermore, the effect of the shaping process was investigated on the basis of the fracture patterns of high-strength TMT ribbed bars under tensile test [8], [10], [12], [14]. The three types of fracture modes are fracture from a node, fracture from a rib corner, and fracture that is independent of the ribs. Fracture that is independent of the ribs is the typical mode of ductile fracture, whereas the two other fracture modes are not. Nevertheless, these two fracture modes can be categorized as internal ductile fractures. Although these fracture modes have different shapes and forms on the surface area of the rib that attenuate the brittle fracture mechanism, the fracture continues toward the center of the bar and culminates in the roughest area. These are the signs of the ductile fracture mechanism, which was proven by the coalescence of voids on the gray region in the middle with the brittle fracture initiation process at the rib node. In short, the mechanism started at the rib node because of the brittle fracture mechanism but progressed through the ductile core, as indicated by the coarsened chevron.

In this study, tensile test experiments were performed to analyze the effect of the shaping process on three parameters, namely, yield strength, ultimate strength, and percent elongation of the bar. This work used random samples of three initial diameters of deformed bars (i.e. BJTS40, certified by industries). The samples were taken randomly from a local distributor in the Greater Jakarta area. According to the standard [15], BJTS40 is a deformed bar type of steel with minimum yield strength of 40 kgf/mm^2 (390 MPa) and minimum ultimate strength of 57 kgf/mm^2 (560 MPa). For each diameter, tensile tests were conducted on the *shaped (S)* and *non-shaped* samples (*NS*). To verify the effect of the shaping process, the tensile test results of plain bars (i.e. BJTP24 Ø10, certified by industries) were also examined. According to the standard [15], BJTP24 is a plain bar type of steel with minimum yield strength of 24 kgf/mm^2 (235 MPa) and minimum ultimate strength of 39 kgf/mm^2 (380 MPa). These conditions were selected to prove that the machine used for the tensile test in the laboratory obtained consistent results. Both grades BJTS40 and BJTP24 are categorized as carbon steel [15]. The results of the tests are interesting. The failure modes of the samples are also determined to verify the conditions selected for the tests. The results of this study can be used as an information resource in engineering practice.

2. Materials and Methods of the Experiment

In this research, the samples used for the tensile tests are grade BJTP24 (plain bars) and grade BJTS40 (deformed bars). For the plain bars (BJTP24 Ø10), eight samples with the diameter of 10 mm were used (in this article, BJTP24 Ø10 means plain steel bar with the diameter of 10 mm and the grade of 24, according to the national standard [15]). This type of sample was selected as it is often used as transverse reinforcement in RC structures. Furthermore, for the deformed bars (BJTS40), three different diameters (i.e. D_0 = 10, 13, 16 mm) were employed (BJTS40 D10 means deformed steel bar with the diameter of 10 mm and the grade of 40, according to the national standard [15]). These three diameters were selected because they are often utilized in two-story houses and low-rise buildings using RC material.

According to the SNI, "D" is used to denote the diameter of the deformed bar and the symbol "Ø" is used to denote the diameter of the plain bar.

These experiments used 7 samples of BJTS40 D10, 10 samples of BJTS40 D13, 5 samples of BJTS40 D16 Fabrication-*x*, and 5 samples of BJTS40 D16 Fabrication-*y* for a total of 27 samples. Despite random sampling, sample BJTS40 D16 was distinguished into two different fabrications (i.e. from two different factories), namely, Fabrication-*x* and Fabrication-*y*.

Each sample, whether the plain or deformed bar, was 1 m in length and was cut into two sides called sides A and B. In particular, for the plain bar (BJTP24 Ø10 mm), both sides were tested without being subjected to the shaping process. By contrast, for the deformed bar, Side A was tested as it was and referred to as the *NS*, whereas Side B was shaped following the national standard [5] and referred to as the *S*. The shaping or machining process was performed separately by the same machine and operator and resulted in three different diameters from the initial diameter D_0 (D = 8, 10, and 12 mm). The test results for the *shaped* and *non-shaped* bars were compared and investigated to analyze the influence of the shaping process.

Table 1. Summary of the Details of the Specimens

Sample	Number of Samples	
	Shaped	Non-shaped
BJTP24 Ø10 mm (plain bar)	–	16
BJTS40 D_0 10 mm (deformed bar)	7	7
BJTS40 D_0 13 mm (deformed bar)	10	10
BJTS40 D_0 16 mm (deformed bar)		
Fabrication-*x*	5	5
Fabrication-*y*	5	5

Figure 1. Universal Testing Machine (UTM) used in this Research

Tensile tests were conducted at room temperature according to ASTM A370 [16, p. 370] and SNI 07 2529 1991 [5] using a Universal Testing Machine (UTM) GOTECH AI-7000-LA20 with 20 tons of capacity. The machine is calibrated once every 6 months. Two sizes of grips i.e. grip for 8–12 mm diameter and grip for 12–16 mm diameter, were used. In addition, a loading rate of 1.15–11.5 MPa/s was applied and controlled when determining yield properties, as regulated by the ASTM [17, p. 8]. Figure 1 shows the condition of the UTM used for the tests. Meanwhile, Table 1 summarizes the details of the specimens. The three parameters measured during the tensile tests were ultimate tensile strength, yield strength, and percent elongation.

3. Statistical and Measurement Uncertainty Analyses of the Materials and Methods of the Experiment

To assess the effect of the shaping process on the accuracy of the tensile test results, the statistical analysis included the calculation of the average ($\bar{x}$), standard deviation (σ), standard uncertainty (u_s), and variability (b) using Equations (1) to (4) on the basis of the results of the tensile tests of steel [18–23]. Inconsistencies in the measured results can be identified by measurement uncertainty analysis [18]. In this case, the variability of the samples was investigated to determine the influence of the shaping process on the variation of the data of the three groups. The three parameters analyzed during the tensile tests were ultimate tensile strength, yield strength, and percent elongation.

Average

$$\bar{x} = \frac{1}{n}\sum_{i=1}^{n} x_i \quad (1)$$

Standard Deviation

$$\sigma = \sqrt{\frac{\sum_{i=1}^{n} x_i - \bar{x}}{(n-1)}} \quad (2)$$

Standard Uncertainty

$$u_s = \frac{\sigma}{\sqrt{n}} \qquad (3)$$

Variability

$$b = \left(\frac{x_{max} - x_{min}}{\bar{x}}\right) 100 \qquad (4)$$

4. Results and Discussion

Plain bars. Tensile test was performed on BJTP24 Ø10 (i.e. the plain bar with the diameter of 10 mm) to determine its ultimate tensile strength, yield strength, and percent elongation. Normally, there should be no difference results of yield and ultimate strengths as the conditions for both sides of the plain bar were the same. Figure 2 shows the tensile test results for all 16 bars. Each curve is labeled with Ø10 followed by the sample number. As shown in Figure 2, the stress–strain curve has a similar trend. This curve shows the obvious yield plateau before reaching the ultimate region. The values of yield and ultimate strength are nearly the same for all samples. However, there is an apparent variation in the results of percent elongation, and the value of the coefficient of variation of percent elongation is 6.92%. Table 2 summarizes the test results of the plain bar samples. The variability of percent elongation is sufficiently high, reaching 22.46%. The current applicable standards in Indonesia, i.e. ACI 318 [24] and SNI 2847: 2013 [25], regulate the variations in the results of the concrete compressive test to an acceptable value of 10%. In this case, as the bar is applied and cast inside the concrete, the authors selected the value of 10% as the acceptable criterion for the variations.

The failure points of the 16 samples of BJTP24 Ø10 occurred in different locations, as shown in Figure 3. The results of the experiments show that, for two samples that come from one bar, the failure modes can be different. The sample from Side A could fail in the middle of the grip, whereas the sample from Side B could fail near the grip. Moreover, BJTP24 Ø10 has a *nearly cup-and-cone* failure mode, as shown in Figure 4. These failure modes are in accordance with the typical fracture of ductile materials [12]–[14].

Table 2. Summary of the Test Results of BJTP24 Ø10 mm

	Yield Strength (MPa)	Ultimate Strength (MPa)	Percent Elongation
$\bar{x}$	381.68	550.41	34.49
Max	390.07	556.56	38.43
Min	372.65	537.87	30.69
Range	17.42	18.69	7.75
σ	5.41	5.15	0.02
b	4.56%	3.40%	22.46
μ	1.42%	0.93%	7.20
u_s	1.35	1.29	0.62

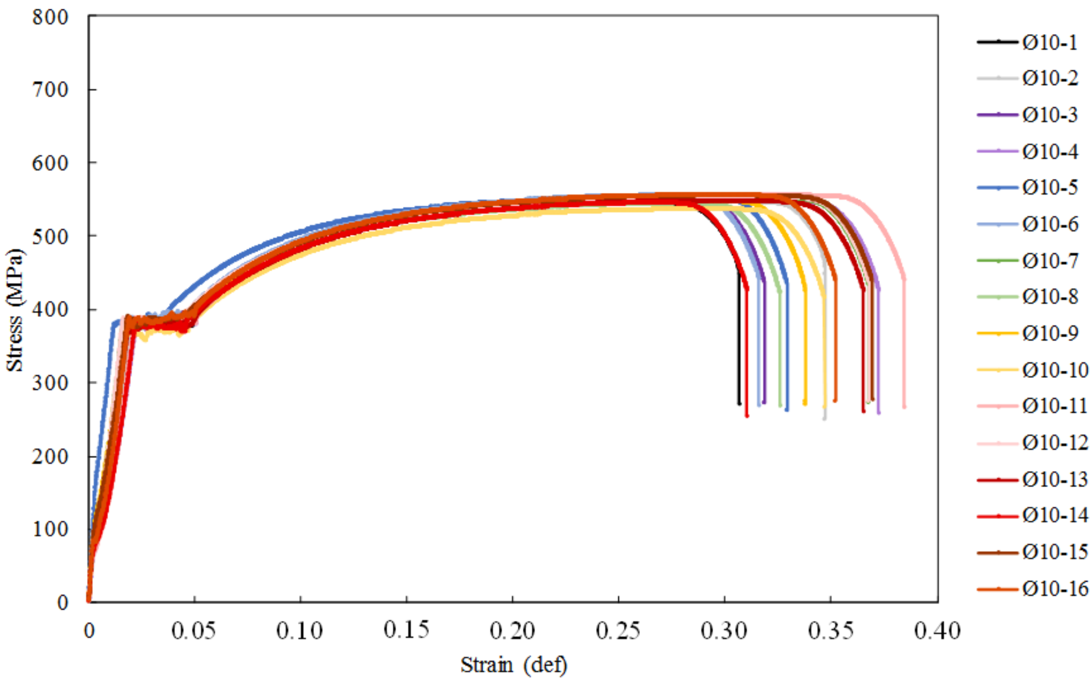

Figure 2. Stress–Strain Curve of BJTP24 Ø10 (Plain Bar with the Diameter of 10 mm)

(a)

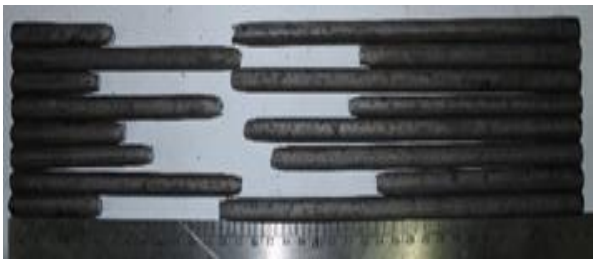

(b)

Figure 3. Fracture Location of BJTP24 Ø10: (a) Side A and (b) Side B

(a)

(b)

Figure 4. Type of Fracture Observed on the Sample BJTP24 Ø10 mm: Nearly Cup-and-Cone

Deformed 7. Figures 5, 6, and 7 show the stress–strain curve test results of the samples BJTS40 D10, BJTS40 D13, and BJTS40 D16. From these curves, the ultimate tensile strength, yield strength, and percent elongation are determined. In Figures 5 and 6, the curves illustrate the behavior of the *S* and *NS* samples, which are presented in red and blue, respectively. Each curve is labeled with D10 or D13 followed by the sample number and condition of the specimen, i.e. whether S or NS. Moreover, in Figure 7, the test results of Fabrication-*x* are presented in red (for *S*) and blue (for *NS*), whereas the test results of Fabrication-*y* are presented in pink (for *S*) and green (for *NS*). Each curve is labeled with D16 followed by the sample number and condition of the specimen, whether Fabrication-*x* or Fabrication-*y*. In general, the yield plateau for the *S* is shorter than that for the *NS*.

Figures 5, 6, and 7 show that, in general, the shaping process affected the strain (percent elongation) of the sample. Thus, the bar from the *NS* can be considered to be more ductile than that from the *S*. An exceptional condition is shown in Figure 7, i.e. for BJTS40 D13, it seems that the results of the *S* and *NS* are not so different. Nevertheless, the difference in the strain is visible. The S (range, 13.73 MPa; coefficient of variation, 11.17%) have a higher coefficient of variation than the *NS* (range, 9.85 MPa; coefficient of variation, 6.80%). The coefficient of variation shows the extent of variability in relation to the average of the samples. The statistical analysis data of the three types of samples are presented in Tables 3, 4, and 5. From these tables, the details of each condition and/or sample will be discussed in the subsequent sections.

As shown in Table 3, the yield strength of BJTP24 Ø10 is the lowest among all of the samples as it is a plain bar (grade BJTP24). For sample BJTS40 D10, the average value of the yield strength of the *S* is slightly higher than that of the *NS* (10.76 MPa). Meanwhile, for the other diameters, i.e. samples BJTS40 D13, BJTS40 D16 Fabrication-*x* (D16-*x*), and BJTS40 16 Fabrication-*y* (D16-*y*), the average value of the yield strength of the *NS* was larger than that of the *S*, with the difference of 16.28 MPa (3.14%), 20.51 MPa (4.34%), and 42.39 MPa (8.46%), respectively. The percentage difference is calculated by dividing the difference between the yield strengths of the *NS* and *S* by the average of their values.

Regarding the range of values of the obtained yield strength, BJTS40 D10S, D13S, and D16S-*x* are the three groups of samples with the largest range at 66.59, 49.63, and 34.12 MPa, respectively (see Table 3). Moreover, in this case, for the sample with the largest range, the coefficient of variation is also high. The sample that underwent the shaping process has a large range of values, and the coefficient of variation is also high (4.33%, 2.82%, and 2.72% for D10S, D13S, and D16S-*x*, respectively). For D16 Fabrication-*y*, the *S* (1.10%) also has a higher coefficient of variation than the *NS* (0.45%). Thus, it is clear that the shaping process can increase the value of the coefficient of variation. In other words, the higher the value of variability is, the lower the accuracy.

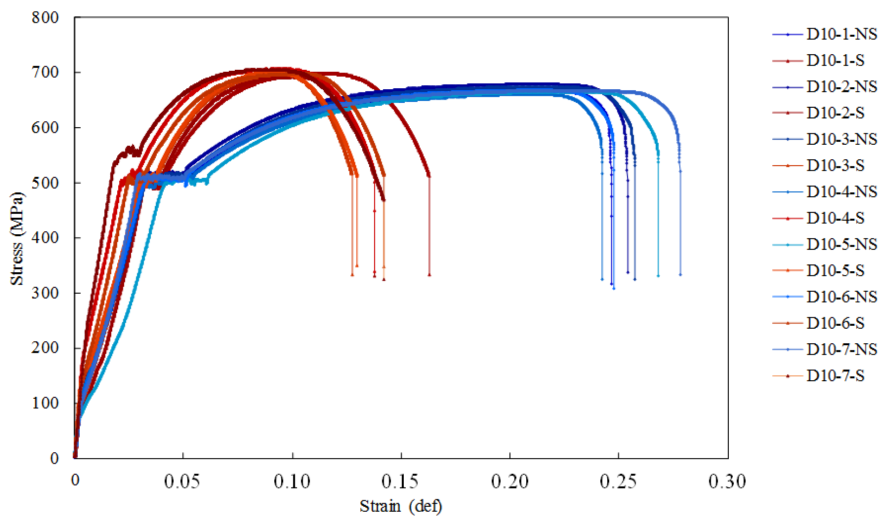

Figure 5. Stress–Strain Curve of the BJTS40 D10 (Deformed Bar) Shaped and Non-shaped Samples

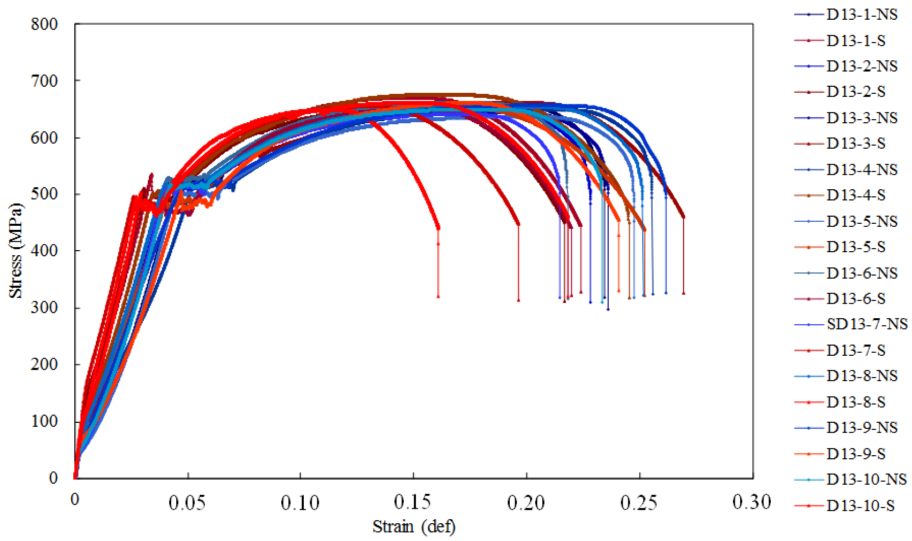

Figure 6. Stress–Strain Curve of the BJTS40 D13 (Deformed Bar) Shaped and Non-shaped Samples

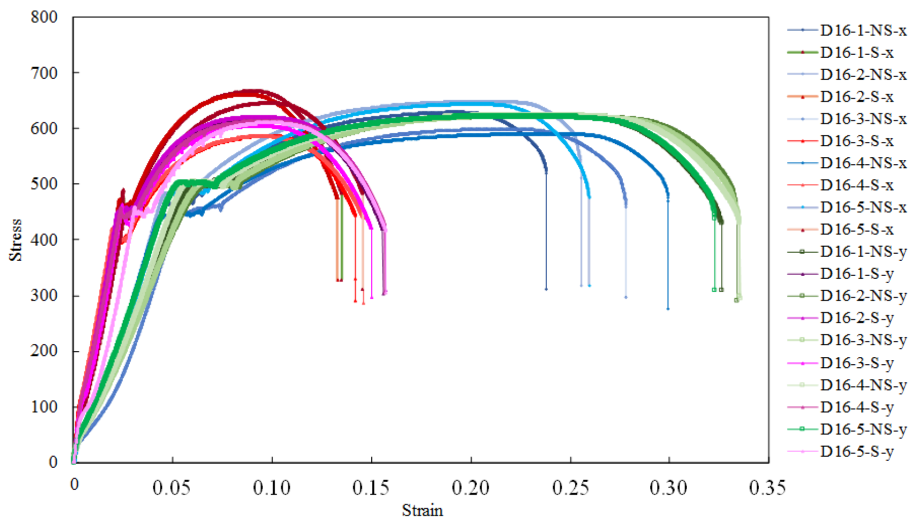

Figure 7. Stress–Strain Curve of the BJTS40 D16 (Deformed Bar) Shaped and Non-shaped Samples (Fabrication-*x* and Fabrication-*y*)

The ultimate tensile strength exhibited the same trend as the yield strength. BJTP24 Ø10 has the lowest value among all samples (see Table 4). Among the four types of samples (D10, D13, D16-*x*, and D16-*y*), only the ultimate strength of D16-*y* shows the same tendency as its yield strength, and the obtained average value of the ultimate strength of the *S* is smaller than that of the *NS* at 9.54 MPa (1.53%). Regarding the range of values of ultimate strength, BJTS40 D10S, D13S, and D13NS are the three groups of samples with the largest range at 49.48, 27.30, and 24.08 MPa, respectively. These results indicate that the *NS* also have a large range of values for the coefficient of variation and variability. However, from these four groups, the majority of the *S* have large range of values.

Tables 3 and 4 show that, in general, the values of the standard deviation (σ) and variability (b) of the *S* (BJTS sample followed by the "*S*" notation) are larger than those of the *NS* (BJTS sample followed by the "*NS*" notation and BJTP sample). This means that the results of the *NS* are more consistent than the results of the *S*.
In the case of percent elongation, the *NS* have higher percent elongation than the *S*. The difference in the average percent elongation between these two types of samples can reach up to 17.54% for BJTS40 D16 Fabrication-*y*, followed by BJTS40 D16 Fabrication-*x* and BJTS40 D10 at 13.79% and 11.15%, respectively. The sample BJTS40 D13S has the largest range for elongation and the highest coefficient of variation. Of all the samples, only in the sample BJTS40 D16 Fabrication-*x* was the coefficient of variation of the *NS* higher than that of the *S* (see Table 5). Table 5 also shows that the coefficient of variation (μ) of the *S* (BJTS sample followed by the "S" notation) are higher than that of the *NS* (BJTS sample followed by the "*NS*" notation and BJTP sample). This means that the results of the *NS* are more consistent than the results of the *S*.

The fracture location of all samples is shown in Figure 8. Most of the *NS* failed near the grip. In the case of the *S*, all types of rebar failed in the middle where the shaping/machining, forming, and lathing processes had occurred. A material is supposed to fail in the weakest zone of the sample. In the case of the *S*, the sample itself was already in the disturbed condition. The shaping process leads to the weakening of a certain zone of the sample. By contrast, in the case of the *NS*, during the tensile test, the bar was elongated along its length. At the exact moment at which the elongation centralizes the failure in the weakest zone, the bas will break. Thus, it is normal for the failure in the *NS* to occur randomly in the area of tension.

The failure modes of the *NS* and *S* are shown in Figure 9. The *NS* of all diameters of the rebar exhibited the shear-and-brittle fracture, which began at the node or rib corner. This condition is in accordance with that observed in the study conducted by Christopher [12]. The *S* of all diameters of the rebar exhibited the nearly cup-and-cone fracture.

Table 3. Summary of the Statistical Data of Yield Strength

	BJTP24 Ø10	**BJTS40 D10 NS**	**BJTS40 D10 S**	**BJTS40 D13 NS**	**BJTS40 D13 S**	**BJTS40 D16 NS-*x***	**BJTS40 D16 S-*x***	**BJTS40 D16 NS-*y***	**BJTS40 D16 S-*y***
n	16	7	7	10	10	5	5	5	5
$\bar{x}$ **(MPa)**	381.68	507.63	518.38	518.37	502.09	472.14	451.63	500.90	458.51
$\Delta\bar{x}$ **(MPa)**	–	10.76 (2.12%)		16.28 (3.14%)		20.51 (4.34%)		42.39 (8.46%)	
Min (MPa)	372.65	493.30	497.94	507.65	486.67	465.29	436.07	497.41	450.34
Max (MPa)	390.07	518.53	564.53	530.21	536.29	477.56	470.20	503.29	463.53
Range (MPa)	17.42	25.22	66.59	22.56	49.63	12.27	34.12	5.88	13.19
σ **(MPa)**	5.41	9.01	22.42	6.89	14.16	5.14	12.30	2.25	5.03
b **(%)**	4.56	4.97	12.85	4.35	9.88	2.60	7.56	1.17	2.88
μ **(%)**	1.42	1.77	4.33	1.33	2.82	1.09	2.72	0.45	1.10
u_s **(MPa)**	1.35	3.40	8.47	2.18	4.48	2.30	5.50	1.01	2.25

Note: *BJTP24 Ø = plain bar; BJTS40 D = deformed bar; S = shaped; NS= Non-shaped; -x = fabrication from factory x; -y = fabrication from factory y*

Table 4. Summary of the Statistical Data of Ultimate Strength

	BJTP24 Ø10	BJTS40 D10 NS	BJTS40 D10 S	BJTS40 D13 NS	BJTS40 D13 S	BJTS40 D16 NS-*x*	BJTS40 D16 S-*x*	BJTS40 D16 NS-*y*	BJTS40 D16 S-*y*
n	16	7	7	10	10	5	5	5	5
$\overline{x}$ **(MPa)**	550.41	668.48	704.33	650.51	660.19	628.68	632.21	622.68	613.14
$\Delta\overline{x}$ **(MPa)**	–	35.85 (%)		9.67 (1.49%)		3.53 (0.56%)		9.54 (1.53%)	
Min (MPa)	537.87	659.61	691.93	637.65	649.74	620.32	626.51	621.92	604.70
Max (MPa)	556.56	677.76	741.41	661.73	677.05	635.15	639.94	623.50	621.25
Range (MPa)	18.69	18.15	49.48	24.08	27.30	14.83	13.42	1.57	16.55
σ **(MPa)**	5.15	5.72	16.87	7.77	8.54	5.39	5.58	0.61	6.17
b **(%)**	3.40	2.71	7.02	3.70	4.14	2.36	2.12	0.25	2.70
μ **(%)**	0.93	0.86	2.40	1.19	1.29	0.86	0.88	0.10	1.01
u_s **(MPa)**	1.29	2.16	6.38	2.46	2.70	2.41	2.50	0.27	2.76

Note: *BJTP24 Ø = plain bar; BJTS40 D = deformed bar; S = shaped; NS = Non-shaped; -x = fabrication from factory x; -y = fabrication from factory y*

Table 5. Summary of the Statistical Data of Percent Elongation of All Samples

	BJTP24 Ø10	BJTS40 D10 NS	BJTS40 D10 S	BJTS40 D13 NS	BJTS40 D13 S	BJTS40 D16 NS-*x*	BJTS40 D16 S-*x*	BJTS40 D16 NS-*y*	BJTS40 D16 S-*y*
n	16	7	7	10	10	5	5	5	5
$\overline{x}$ **(%)**	32.70	25.14	13.99	23.80	22.43	27.82	14.02	33.07	15.53
$\Delta\overline{x}$ **(%)**	–	11.15		1.37		13.79		17.54	
Min (%)	30.69	23.39	12.73	21.44	16.11	25.55	13.28	32.30	14.99
Max (%)	34.72	27.79	16.27	26.15	26.93	29.94	14.59	33.54	15.73
Range (%)	4.03	4.41	3.54	4.71	10.82	4.40	1.31	1.24	0.73
σ **(%)**	2.08	1.40	1.15	1.57	3.06	1.62	0.60	0.57	0.30
b **(%)**	12.32	17.52	25.31	19.78	48.25	15.80	9.31	3.75	4.73
μ **(%)**	6.36	5.55	8.25	6.59	13.63	5.83	4.30	1.72	1.96
u_s **(%)**	0.52	0.53	0.44	0.50	0.97	0.73	0.27	0.25	0.14

Note: *BJTP24 Ø = plain bar; BJTS40 D = deformed bar; S = shaped; NS = Non-shaped; -x = fabrication from factory x; -y = fabrication from factory y*

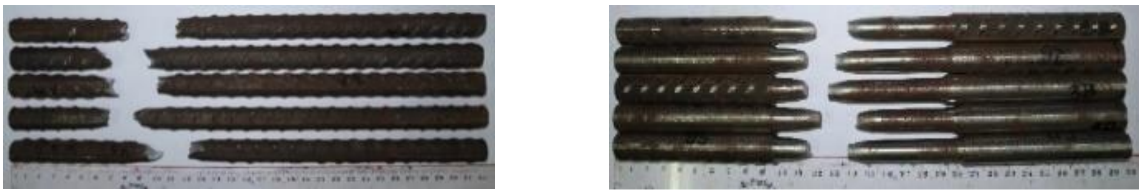

(a)

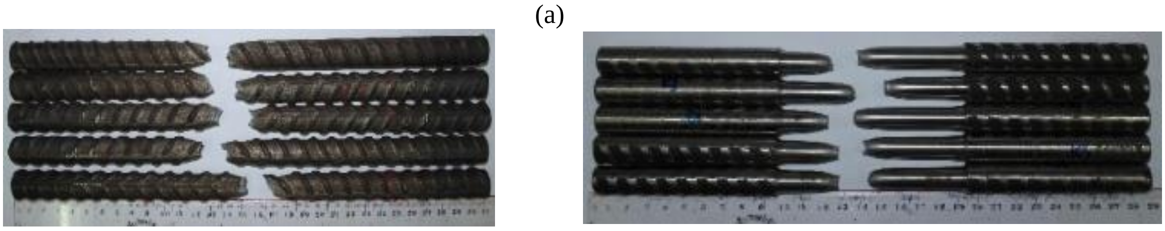

(b)

Figure 8. Fracture Location of BJTS40 Non-shaped and Shaped samples: (a) D16 Fabrication-*x* and (b) D16 Fabrication-*y*

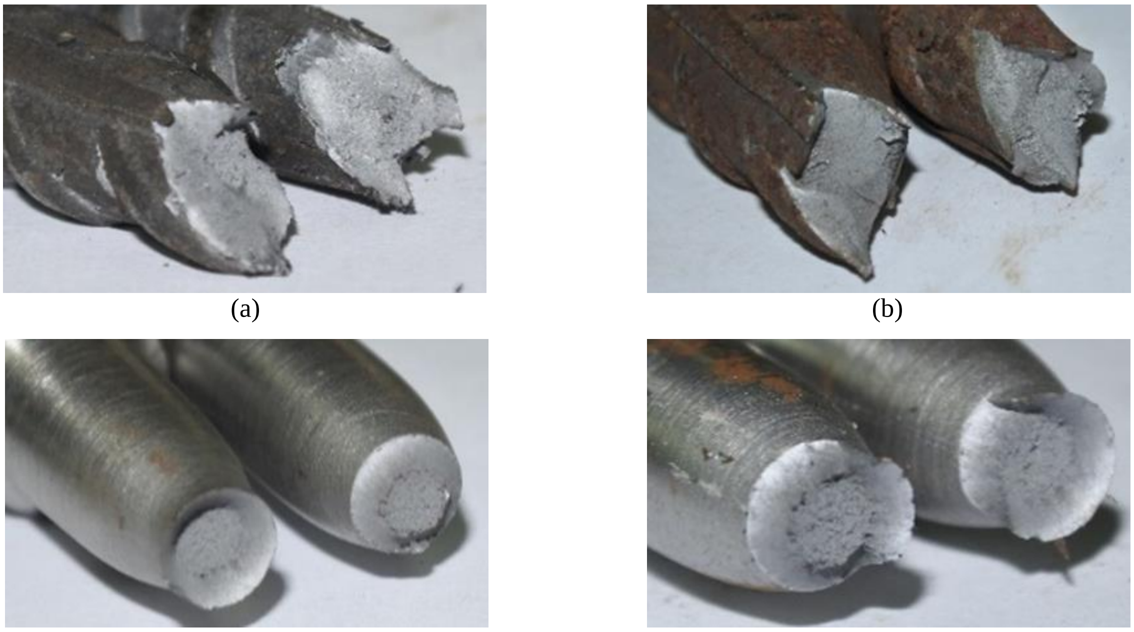

(a) (b) (c) (d)

Figure 9. Type of Fracture Observed on the Sample BJTS40: (a) Non-shaped Type 1, (b) Non-shaped Type 2, (c) Shaped Type 1, and (d) Shaped Type 2

5. Conclusion

In conclusion, the results of the tensile tests of *S* and *NS* from the same bar length show the significant effects of the forming, shaping/machining, and lathing processes. Despite the fact that the machine used for the shaping process was operated by one person, different results were obtained. The stress–strain curve of the *NS* and *S* can be easily distinguished, except for the case of sample BJTS40 D13. In general, the yield plateau for the *S* is shorter than that for the *NS*. The *NS* have a higher percent elongation than the *S*. Moreover, the failure of the *S* is concentrated on the machined part; thus, the fracture always occurs in the shaped area. Meanwhile, the *NS* can fail near the grip or in the middle of the body of the bar. The type of fracture observed on the *S* of the rebar is the nearly cup-and-cone fracture, whereas that on the *NS* of the rebar is the shear-and-brittle fracture.

Intentionally “disturbing” the sample in the shaping process significantly affected the variability. In all cases (elongation, yield strength, and ultimate strength), the *S* mostly had a higher coefficient of variation than the *NS*. Statistically, all of the bars had yield and ultimate strengths with a coefficient of variation lower than 5%. Meanwhile, in the case of percent elongation, the coefficient of variation reached 13.63% (type BJTS40 D13-S), which is higher than 10%, although the conditions for the test (i.e. loading rate, the preparation, and bar length) were kept the same. The 10% threshold of the coefficient of variation is important in the application of the bar cast in concrete to form RC. The current applicable standards in Indonesia, i.e. ACI 318 [24] and SNI 2847: 2013 [25], regulate the variations in the results of the concrete compressive test to an acceptable value of 10%. Thus, in engineering practice, the tensile test results of the *NS* are more consistent than the results of the *S*.

Regarding the results of this study, if the information on the elongation of the bar is deemed important, then it is recommended that the test be performed without the shaping process. Otherwise, the results may not be accurate.

References

[1] J.C. McCormac, R.H. Brown, Design of Reinforced Concrete 10th Edition, Wiley, 2013.
[2] H. Rathod, K. Parmar, Comparison of a Rebar with a Plain Surface and a Deformed Axis over HYSD Rebars, 2012.
[3] J.K. Wight, J.G. MacGregor, Reinforced Concrete: Mechanics and Design, 6th edition. Upper Saddle River, N.J: Prentice Hall, 2011.
[4] S. Somayaji, Civil Engineering Materials. Prentice Hall, 2001.
[5] Badan Standarisasi Nasional, SNI 07-2529–1991 Metode Pengujian Kuat Tarik Baja Beton, BSN, Jakarta, 1991.
[6] American Society of Testing Material ASTM International, ASTM E8/E8M–04 Standard Test Methods for Tension Testing of Metallic Materials, ASTM, Philadelphia, 2016.

[7] Krakatau Steel KS, PT KRAKATAU STEEL (Persero) Tbk.
[8] M. Mukherjee, C. Dutta, A. Haldar, Mater. Sci. Eng. A, 543 (2012) 35.
[9] A.T. Wibowo, Undergraduate Thesis, Civil Engineering Study Program, Faculty of Engineering, Universitas Muhammadiyah Surakarta, Surakarta, 2011.
[10] L.T. Lestari, M.S. Sitorus, H.A. Lie, S. Tudjono, Konferensi Nasional Teknik Sipil 12, Batam, 2018.
[11] J. Lemaitre, J.-L. Chaboche, Mechanics of Solid Materials, Cambridge University Press, 1990.
[12] S. Christopher, Trends Mech. Eng. Technol. 5 (2015) 8.
[13] J. Lemaitre, Handbook of Materials Behavior Models, ScienceDirect, 2001.
[14] I.R. Kabir, M.A. Islam, Am. J. Mech. Eng. 2/1 (2014) 8.
[15] Badan Standarisasi Nasional, SNI 2052:2014 Baja Tulangan Beton, BSN, Jakarta, 2014.
[16] American Society of Testing Material ASTM International, ASTM A370–18 Test Methods and Definitions for Mechanical Testing of Steel Products, ASTM, Philadelphia, 2018.
[17] American Society of Testing Material ASTM International, ASTM E8/E8M–16a Standard Test Methods for Tension Testing of Metallic Materials, ASTM, Philadelphia, 2016.
[18] B. Podgornik, B. Žužek, M. Sedlaček, V. Kevorkijan, B. Hostej, Meas. Sci. Rev. 16 (2016) 1.
[19] M. Désenfant, M. Priel, Meas. 39/9 (2006) 841.
[20] H. Imai, Meas. 46/8 (2013) 2942.
[21] S.F. Beckert, G. Domeneghetti, D. Bond, Meas. 51 (2014) 420.
[22] D. Kuhinek, I. Zorić, P. Hrženjak, Meas. Sci. Rev. 11/4 (2011) 112.
[23] S. Kłysz, J. Lisiecki, Tech. Sci. 11 (2008) 265.
[24] American Concrete Institute Committee 318, ACI 318-19: Building Code Requirements for Structural Concrete and Commentary, ACI, Farmington Hills, 2019.
[25] Badan Standarisasi Nasional, SNI 2847-2013 Persyaratan Beton Struktural untuk Bangunan Gedung, BSN, Jakarta, 2013.